

Propagation of reflective three-output with dual-layered grating in second-order Littrow configuration

ZEFAN LIN, BO WANG*, ZHISEN HUANG, WENHUA ZHU, YONGCHUN ZHOU, LICHANG LI, ZHIPENG LI, GUOYU LIANG, JIAMAN HONG

School of Physics and Optoelectronic Engineering, Guangdong University of Technology, Guangzhou 510006, China

A novel type of three-output dual-layered reflective grating is proposed in this paper. Through rigorous coupled-wave analysis, the appropriate thickness of two dielectric layers in grating region can be calculated. According to the optimization results, when the incident light with wavelength 1550 nm is incident at the second Bragg angle, the grating can diffract the incident light energy to the three orders, and the efficiency is close to 33%. Compared with the reported three-output grating under the second Bragg angle incidence, the dual-layered grating has higher diffraction efficiency and better incident angle bandwidth for TE-polarized light.

(Received September 2, 2020; accepted February 14, 2023)

Keywords: Three-output propagation, Dual-layered grating, High efficiency

1. Introduction

The propagating gratings are more suitable for miniaturization and integration, and are widely used in various laser systems [1-6], such as the absorber [7-9], beam splitter [10-12], coupler [13-16], nonreciprocal thermal emitter [17], surface-enhanced Raman scattering [18,19], measurement [20], interferometer [21] and so on. Beam splitters are key elements in various applications [22-26]. For decades, the grating diffraction theory has formed a relatively perfect theoretical system through the efforts of researchers [27-29]. By optimizing the grating structure parameters, such as grating period, grating depth, duty cycle and refractive index of grating material, the suitable grating diffraction efficiency can be obtained. Due to the satisfying performance and relatively simple structure, metamaterial has been widely used in optical systems [30-35]. It may be made of metal or dielectric materials deposited on the substrate by etching. Before fabrication, the required grating parameters should be defined.

For high-density gratings with rectangular grooves, the modal method has a simple physical understanding of the interference in the gratings [27]. By explaining the diffraction process, the simplified modal method can provide a basis for evaluating reflective efficiency and grating depth in theory. The rigorous coupled-wave analysis (RCWA) is a suitable method to optimize the grating profile, which can calculate the appropriate grating parameters [28]. In order to achieve the goal of designing high efficiency three-output grating, we should adopt the RCWA method to optimize the grating

parameters. Whether for TE-polarized light or for TM-polarized light, an excellent three-output grating should have a diffraction efficiency of more than 30% per order and a diffraction efficiency ratio close to 1. As far as we know, no one has ever designed the dual-layered grating based on metal-mirror configuration with operating wavelength of 1550 nm at the second Bragg angle.

In this paper, the dual-layered grating based on metal-mirror configuration is proposed for three-output beam splitter. The RCWA method is used to optimize the grating parameters so that the diffraction efficiency of TE-polarized light and TM-polarized light can be divided into three orders. Compared with the existing three-output grating with the special duty cycle of 0.6 [36], the new grating has better beam splitting performance for the usual duty cycle of 0.5.

2. Propagation analysis and optimization

Fig. 1 describes the schematic of the surface-relief dual-layered reflective grating under the second Bragg angle incidence. The novel grating is composed of two grating layers, a metal reflective layer and a fused-silica substrate with excellent optical performance [37-41]. The groove of grating is air with refractive index of $n = 1.0$. The grating rectangular ridge can be comprised of two kinds of dielectric materials with two different etching depths. The first layer and substrate of the grating are fused silica with refractive index of $n_1 = 1.45$. The material of the second layer is chosen as Ta_2O_5 with the

refractive index of $n_2 = 2.0$. In the grating geometrical parameters, each thickness of two gating layers is h_1 and h_2 , respectively. In addition, the period of the grating is d and the duty cycle is defined as the ratio of ridge width to period. And the metal reflective layer is silver with a refractive index of $n_m = 0.469-9.32i$ and the thickness of h_m . Since the parameters of the TE-polarized grating and the TM-polarized grating are different. Therefore, we use the subscripts to measure the parameters of different gratings. For example, h^{TE} and h^{TM} are the grating ridge depths of TE polarization and TM polarization,

respectively. A plane wave illuminates the grating with an incident angle $\theta = \sin^{-1}(\lambda/nd)$, and the incident wavelength is $\lambda = 1550$ nm. The TE-polarized light and TM-polarized light can be coupled into different propagation directions by grating, and output to the diffraction orders, where the propagating direction can be determined by the grating equation. The coupled diffraction orders can be only set to the -2nd order, the -1st order and the 0th order within the grating period range of $\lambda - 2\lambda$.

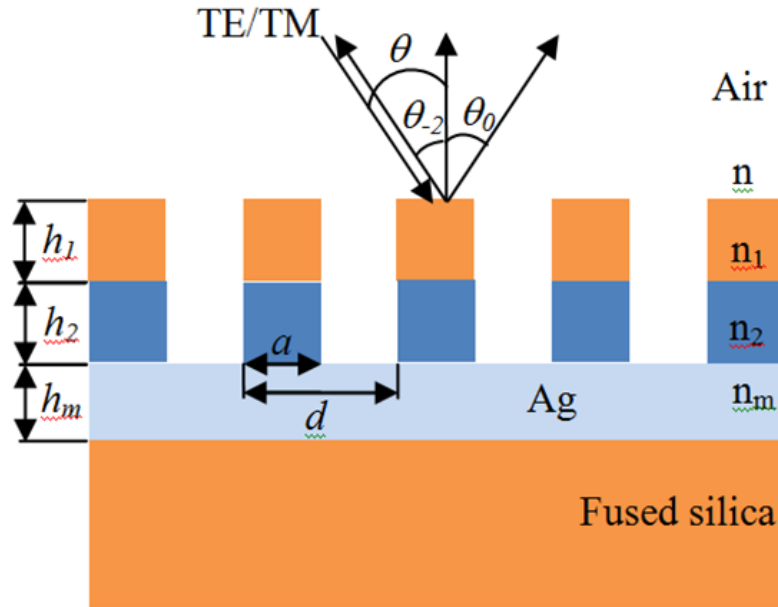


Fig. 1. Schematic of the surface-relief dual-layered reflective grating under the second Bragg incidence (color online)

When the thickness of the metal plate exceeds $0.1 \mu\text{m}$, complete reflection of incident light can be approximately achieved. For ease of manufacturing, we set the duty cycle to 0.5. We numerically optimize the grating layer thickness h and grating period according to the RCWA method. In addition, before the grating is put into mass production, it is necessary to obtain appropriate grating profile parameters, including grating period and thickness of two grating layers. RCWA method can be used effectively to optimize the new grating. After some calculations, the grating period d is set to 1601 nm.

Fig. 2 shows efficiencies of the 0th order, the -1st order and the -2nd order versus the grating the thicknesses of h_1 and h_2 for TE and TM polarizations with a duty cycle of 0.5 and period of 1601 nm under the second Bragg angle incidence.

According to Fig. 2, when the thickness of the first layer h_1^{TE} is $1.72 \mu\text{m}$ and thickness of the second layer h_2^{TE} is $1.68 \mu\text{m}$, the grating can divide the TE-polarized light into three orders of 0th order, -1st order and the -2nd order, and the diffraction efficiencies are 32.89%, 32.90%, 32.97%, respectively, and the sum of the three reflection efficiencies exceeds 98%. For TM polarization, with the optimized depth $h_1^{TM} = 0.71 \mu\text{m}$ and thickness of $h_2^{TM} = 1.13 \mu\text{m}$, diffraction efficiencies of the 0th order, the -1st order and the -2nd order can reach 31.99%, 32.07% and 32.19%, respectively.

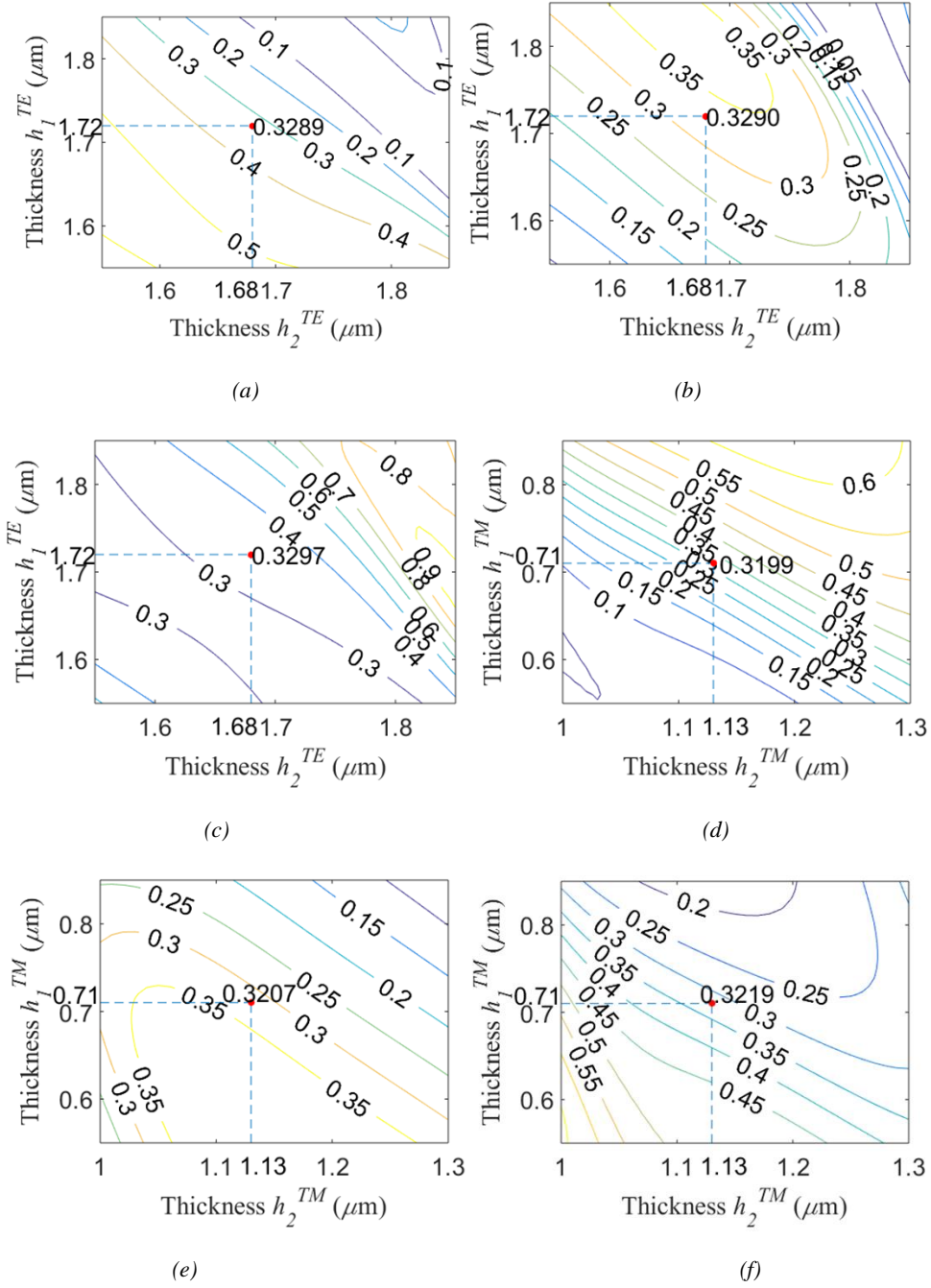


Fig. 2. Efficiencies of the 0th order, the -1st order and the -2nd order versus grating depth and period: (a) TE polarization in the 0th order, (b) TE polarization in the -1st order, (c) TE polarization in the -2nd order, (d) TM polarization in the 0th order, (e) TE polarization in the -1st order, (f) TM polarization in the -2nd order (Color online)

Although RCWA method describes a numerical analysis vector method and provides three order diffraction efficiency values, it cannot give a physical interpretation of the diffraction. In contrast, theoretic modal method can clearly describe the diffraction process. TE- or TM-polarized light can be coupled into some discrete grating modes, where the transition process is called the coupling physical mechanism. Furthermore, the propagating constants are determined by the effective indices, thus, the results of effective indices can be

obtained by settling following dispersion conditions for TE-polarized light [27]:

$$\cos k_1(1-f)d \cdot \cos k_2fd - \frac{k_1^2 + k_2^2}{2k_1k_2} \cdot \sin k_1(1-f)d \cdot \sin k_2fd = \cos \alpha d$$

(1)

and for TM polarization:

$$\cos k_1(1-f)d \cdot \cos k_2fd - \frac{n_2^4 k_1^2 + k_2^2}{2n_2^2 k_1 k_2} \cdot \sin k_1(1-f)d \cdot \sin k_2fd = \cos \alpha d \quad (2)$$

with:

$$k_p = k_0 \sqrt{n_p^2 - n_{eff}^2}, \alpha = k_0 \sin \theta, k_0 = \frac{2\pi}{\lambda} \quad (3)$$

The effective indices for both polarizations are $n_{0eff}^{1TE} = 1.3305$, $n_{1eff}^{1TE} = 0.8325$, $n_{2eff}^{1TE} = 0.6475$, $n_{0eff}^{1TM} = 1.2751$, $n_{1eff}^{1TM} = 0.7472$, $n_{2eff}^{1TM} = 0.7054$, $n_{0eff}^{2TE} = 1.8711$, $n_{1eff}^{2TE} = 1.4425$, $n_{2eff}^{2TE} = 0.8876$, $n_{0eff}^{2TM} = 1.7975$, $n_{1eff}^{2TM} = 1.1476$, $n_{2eff}^{2TM} = 0.9609$. When the waves are reflected back to the grating ridge, the waves are diffracted again. Due to multimode interference, TE and TM polarizations of three diffraction orders can be formed.

It has been noted that the energy exchanging between the incident light and grating modes is depended on the overlap integral for TE polarization [27]:

$$\langle E_y^{in}(x) \leftrightarrow u_q(x) \rangle = \frac{\left| \int_0^{d_{TE}} E_y^{in}(x) u_q(x) dx \right|^2}{\int_0^{d_{TE}} |E_y^{in}(x)|^2 dx \int_0^{d_{TE}} |u_q(x)|^2 dx} \quad (4)$$

For TM polarization, the overlap integral can be expressed as:

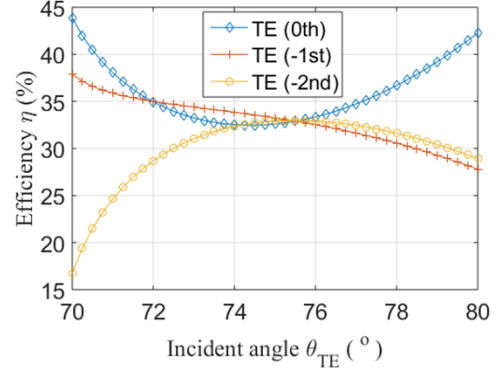
$$\langle H_y^{in}(x) \leftrightarrow u_n(x) \rangle = \frac{\left| \int_0^{d_{TM}} H_y^{in}(x) u_n(x) dx \right|^2}{\int_0^{d_{TM}} |H_y^{in}(x)|^2 dx \int_0^{d_{TM}} |u_n(x)|^2 dx} \quad (5)$$

where the $u_q(x)$ is that of the electric field of the q th grating mode and the $u_n(x)$ is the magnetic field of the n th grating mode. $E_y^{in}(x)$ and $H_y^{in}(x)$ are both the incident waves. In the grating substrate, the grating modes can be coupled into the diffraction orders for both TE and TM polarizations.

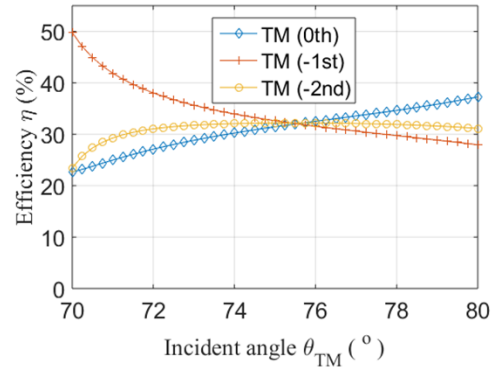
3. Research on the applicable broad working bandwidths

In practical industrial manufacturing, we should consider tolerances in the manufacturing process, such as angle of incidence and grating period etc. Fig. 3 shows the diffraction efficiency with different incident angle for the optimized grating parameters. In Fig. 3, for TE-polarized light, the incident angle is between 72.49°

and 78.46° to ensure that the diffraction efficiencies of the three diffraction orders exceed 30%. To achieve the same goal, for TM-polarized light, the angle of incidence can be between 73.82° and 77.69°.



(a)



(b)

Fig. 3. Diffraction efficiency of the three-output reflective grating versus incident wavelength with the duty cycle of 0.5 near second Bragg angle incidence: (a) TE polarization and (b) TM polarization (color online)

For TM-polarized grating, although the diffraction efficiency of the grating is lower than that of TE-polarized grating, the tolerance of TM-polarized grating is obviously better. Fig. 4 reflects the diffraction efficiency of the optimized grating parameters for different grating periods. In Fig. 4, for TM-polarized light, the grating period in the range of 1589-1616 nm, three diffraction orders can achieve diffraction efficiencies exceeding 30%. Fig. 5 shows the diffraction efficiency with different incident wavelength for the optimized grating parameters. In Fig. 5, although the incident wavelength can be deviated from the central wavelength, the high-efficiency performance can be achieved. For TM-polarized light, the diffraction efficiency of the three diffraction orders exceeds 30%, when the incident wavelength bandwidth is 1536-1559 nm.

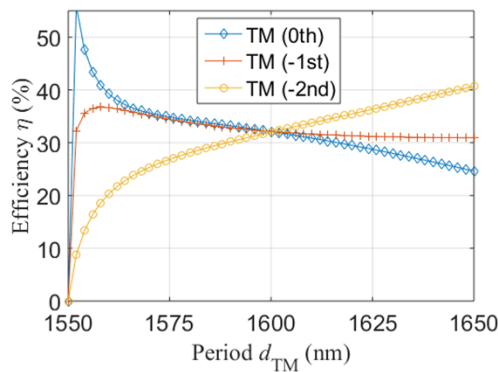


Fig. 4. Diffraction efficiency versus the TM-polarized grating period for a wavelength of 1550 nm under second Bragg angle incidence (color online)

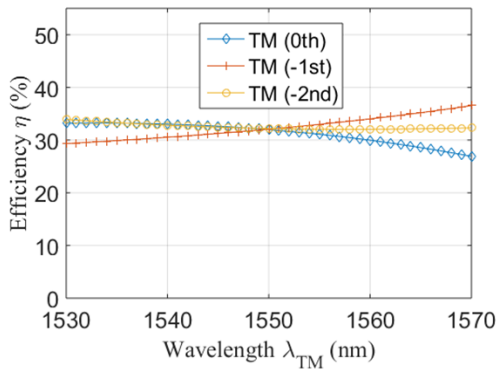


Fig. 5. Diffraction efficiency of the three-output TM-polarized grating versus the incident wavelength under second Bragg angle incidence (color online)

4. Conclusion

In conclusion, the RCWA method is used to design and investigate the reflective three-output grating under second Bragg angle incidence, which improves the diffraction efficiency and wide incident bandwidth. Compared to previous research with special duty cycle of 0.6 [36], the total efficiency for TE polarization can be arrived at 98.76%, for the usual duty cycle of 0.5 by using RCWA. What is more, the beam splitting effect of TE-polarized light is more uniform, the efficiency ratio of -1st order to 0th order can reach 1.0003, and the efficiency ratio of -2nd order to -1st order can reach 1.002. For TE polarization, the wide incident angle bandwidth is 5.97° , and for TM polarization, the wide incident angle bandwidth is 3.87° . The appropriate bandwidth is very important for practical applications.

Acknowledgements

This work is supported by the Science and Technology Program of Guangzhou (202002030284, 202007010001).

References

- [1] M. A. Fiaz, A. Ahmad, M. A. Ashraf, *Waves in Random and Complex Media* **31**(4), 712 (2021).
- [2] W. R. Lopes, P. V. dos Santos, J. G. V. Rocha, J. F. Carvalho, M. T. de Araujo, *Opt. Mater.* **128**, 112445 (2022).
- [3] Z. Qiao, *Optik* **245**, 167668 (2021).
- [4] T. Iqbal, H. Tabassum, S. Afsheen, M. Ijaz, *Waves in Random and Complex Media* **32**(4), 1571 (2022).
- [5] O. Sakhno, L. M. Goldenberg, M. Wegener, C. Dreyer, A. Berdin, J. Stumpe, *Opt. Mater.* **128**, 112457 (2022).
- [6] D. A.B. Therien, N. M. Culum, D. M. McRae, L. Mazaheri, F. Lagugné-Labarthet, *Opt. Mater.* **112**, 110775 (2021).
- [7] X. Zhu, B. Wang, *Opt. Mater.* **133**, 112958 (2022).
- [8] S. L. Mortazavifar, M. R. Salehi, M. Shahraki, *Eur. Phys. J. Plus* **137**(9), 1072 (2022).
- [9] C. Fu, B. Wang, X. Zhu, Z. Xiong, Y. Huang, *Optik* **257**, 168839 (2022).
- [10] Z. Huang, B. Wang, *Opt. Mater.* **125**, 112065 (2022).
- [11] H. Li, T. Huang, L. Lu, Z. Hu, B. Yu, *Opt. Laser Technol.* **145**, 107465 (2022).
- [12] Z. Huang, B. Wang, *Opt. Laser Technol.* **152**, 108102 (2022).
- [13] S. Yang, J. Xu, Y. Li, L. Wu, X. Quan, L. Fu, M. Liu, X. Cheng, *Opt. Mater.* **118**, 111229 (2021).
- [14] D. Zhu, H. Ye, Y. Liu, J. Li, Y. Wang, Z. Yu, *Opt. Laser Technol.* **136**, 106789 (2021).
- [15] J. Cheng, *Opt. Laser Technol.* **148**, 107730 (2022).
- [16] S. F. Haddawi, N. Roostaei, S. M. Hamidi, *Opt. Laser Technol.* **156**, 108577 (2022).
- [17] J. Wu, F. Wu, X. Wu, *Opt. Mater.* **120**, 111476 (2021).
- [18] R. Goel, V. Awasthi, P. Rai, S. K. Dubey, *Opt. Mater.* **122**, 111735 (2021).
- [19] X. Wang, Y. Wu, X. Wen, X. Bai, Y. Qi, L. Zhang, H. Yang, Z. Yi, *Opt. Mater.* **121**, 111536 (2021).
- [20] N. Berberova-Buhova, L. Nedelchev, G. Mateev, E. Stoykova, V. Strijkova, D. Nazarova, *Opt. Mater.* **121**, 111560 (2021).
- [21] S. Nishiwaki, K. Narumi, T. Korenaga, *Sci. Rep.* **9**, 1753 (2019).
- [22] E. Hosseinirad, J. A. Esfahani, F. Hormozi, K. C. Kim, *Eur. Phys. J. Plus* **136**(5), 552 (2021).
- [23] L. Ali, R. ul Islam, M. Imran, M. Ikram, I. Ahmad, *Eur. Phys. J. Plus* **137**(11), 1236 (2022).

- [24] T. Qiu, H. Ma, P. Xin, X. Zhao, Q. Liu, L. Chen, Y. Feng, Z. Yu, *Eur. Phys. J. Plus* **137**(1), 126 (2022).
- [25] P. A. Mohammed, *Opt. Mater.* **112**, 110685 (2021).
- [26] P. Pan, J. Wen, S. Zha, X. Cai, H. Ma, J. An, *Opt. Mater.* **118**, 111250 (2021).
- [27] I. C. Botten, M. S. Craig, R. C. Mcphedran, J. L. Adams, J. R. Andrewartha, *Opt. Acta.* **28**(3), 413 (1981).
- [28] M. G. Moharam, D. A. Pommet, E. B. Grann, T. K. Gaylord, *J. Opt. Soc. Am. A* **12**(5), 1077 (1995).
- [29] Y. Tamura, J. Nakayama, *J. Opt. Soc. Am. A* **35**(8), 1306 (2018).
- [30] Y. Xiong, S. Wen, F. Li, C. Zhang, *Waves in Random and Complex Media* **32**(4), 1862 (2022).
- [31] T. Gric, *Waves in Random and Complex Media* **31**(6), 1246 (2021).
- [32] M. Mohammadi, F. H. Kashani, J. Ghalibafan, *Waves in Random and Complex Media* **31**(6), 1211 (2021).
- [33] Z. Xiao, F. Lv, W. Li, H. Zou, C. Li, *Waves in Random and Complex Media* **31**(6), 2168 (2021).
- [34] B. C. Zhou, D. H. Wang, J. J. Ma, B. Y. Li, Y. J. Zhao, K. X. Li, *Waves in Random and Complex Media* **31**(5), 911 (2021).
- [35] T. Ioannidis, T. Gric, E. Rafailov, *Waves in Random and Complex Media* **32**(1), 381 (2022).
- [36] H. Li, B. Wang, H. Pei, L. Chen, L. Lei, J. Zhou, *Superlattices Microstruct.* **93**, 157 (2016).
- [37] L. Zhang, *Eur. Phys. J. Plus* **136**(11), 1173 (2021).
- [38] H. Talukder, M. H. K. Anik, M. I. A. Isti, S. Mahmud, U. Talukder, S. K. Biswas, B. R. Altahan, L. K. Smirani, S. K. H. Ahammad, A. N. Z. Rashed, *Eur. Phys. J. Plus* **137**(11), 1262 (2022).
- [39] A. Foti, M. G. Donato, O. M. Maragò, P. G. Gucciardi, *Eur. Phys. J. Plus* **136**(1), 30(2021).
- [40] A. Aman, S. Prasad, S. Prakash, G. Sharma, V. Singh, *Waves Random Complex Media* **32**(3), 1048 (2022).
- [41] M. A. Butt, S. N. Khonina, N. L. Kazanskiy, *Waves Random Complex Media* **31**(6), 2397 (2021).

*Corresponding author: wangb_wsx@yeah.net